



HAL
open science

Structural investigations of polymer materials by DNP solid-state NMR

Giulia Mollica, Fabio Ziarelli, Pierre Thureau, Stéphane Viel

► **To cite this version:**

Giulia Mollica, Fabio Ziarelli, Pierre Thureau, Stéphane Viel. Structural investigations of polymer materials by DNP solid-state NMR. *NMR Methods for Characterization of Synthetic and Natural Polymers*, RSC Publishing, pp.533-554, 2019, 978-1-78801-400-7. 10.1039/9781788016483-00533 . hal-02877353

HAL Id: hal-02877353

<https://amu.hal.science/hal-02877353>

Submitted on 2 Sep 2020

HAL is a multi-disciplinary open access archive for the deposit and dissemination of scientific research documents, whether they are published or not. The documents may come from teaching and research institutions in France or abroad, or from public or private research centers.

L'archive ouverte pluridisciplinaire **HAL**, est destinée au dépôt et à la diffusion de documents scientifiques de niveau recherche, publiés ou non, émanant des établissements d'enseignement et de recherche français ou étrangers, des laboratoires publics ou privés.

CHAPTER 21

Structural investigations of polymer materials by dynamic nuclear polarisation solid-state NMR

Giulia Mollica,^a Fabio Ziarelli,^b Pierre Thureau,^a and Stéphane Viel^{a,c,*}

^aAix Marseille Univ, CNRS, ICR, UMR7273, F-13397 Marseille (France)

^bAix Marseille Univ, CNRS, Centrale Marseille, FSCM, FR1739, F-13397 Marseille (France)

^cInstitut Universitaire de France, F-75005, Paris (France)

(*) Corresponding contributor: • E-mail: s.viel@univ-amu.fr

• Mailing address: Aix-Marseille Université

Institut de Chimie Radicalaire
Campus St Jérôme, service 512
Av. Escadrille Normandie Niemen
13397 Marseille cedex 20 (France)

Abstract

Solid-state nuclear magnetic resonance (SSNMR) has established itself as an essential structural elucidation technique in polymer science because it can non-destructively provide unique molecular-level information with atomic resolution on complex macromolecular materials, especially when combined with complementary techniques such as scattering and computer simulation. The Achilles' heel of NMR, however, is its low sensitivity due to the weak nuclear spin polarisation at thermal equilibrium, even at very high magnetic fields. One intriguing way to enhance NMR sensitivity is dynamic nuclear polarisation (DNP), which relies on the microwave-driven transfer of thermal electron spin polarisation to nuclei. DNP is attracting scientific attention owing to the availability of both high-power/high-frequency microwave sources and efficient DNP polarising agents (*i.e.* paramagnetic species used for doping diamagnetic samples to provide the source of electron polarisation for DNP). At moderately high magnetic fields (~ 10 T), large DNP signal enhancements can now be readily obtained, which has led to unprecedented SSNMR applications. In this review, we describe the requirements for high-field DNP SSNMR and provide examples of its use for the structural analysis of organic polymer materials, so as to highlight its advantages and (current) limitations for the field.

21.1. Context and focus

Nuclear magnetic resonance (NMR) has a long history in revealing intricate details on the structure and dynamics of polymers,^{1,2} as testified also by the series of high-quality contributions of this edited book and the references therein. One of the reasons why NMR has become such a powerful analytical and characterisation technique in general, including for the study of polymeric species, undoubtedly lies in its very high resolution, which allows significant spectral features (*e.g.* chemical shifts, coupling constants...) to be unravelled with high accuracy and precision. NMR, however, is also known to be severely limited by its low sensitivity, which requires large amounts of samples to be analysed in order to obtain exploitable NMR signals with measurable intensities. As such, ever since its formal inception in 1946,^{3,4} boosting up the NMR sensitivity has been the goal and subject of intensive research and developments, especially in biomolecular settings.⁵ These have given rise to formidable theoretical, experimental, and technological advances dedicated to enhancing the sensitivity of NMR experiments performed both in the liquid and in the solid states. In this respect, one possible strategy to improve the NMR sensitivity is to increase the intrinsically low nuclear spin polarisation, which results from unfavourable Boltzmann statistics. Such a scheme is generally referred to as hyperpolarisation. Hyperpolarisation has become today a topic of research on its own in the NMR community, fostering a series of distinct methods that aim at boosting up the nuclear spin polarisation in order to exalt NMR sensitivity.⁵ One of these methods is dynamic nuclear polarisation (DNP). While the very concept of DNP was proposed quite a long time ago, in a very famous theoretical paper by Overhauser in 1953,⁶ subsequently followed by an experimental demonstration by Carver and Slichter,⁷ applications of DNP has long remained limited and constrained to relatively low magnetic fields. In fact, apart from a few initial studies performed in the 1960s, which mostly focused on theoretical aspects,⁸⁻¹⁷ DNP has been rather neglected by the global NMR community until the seminal contributions of Ardenkjaer-Larsen at Amersham Health Research Laboratory and Griffin at MIT (together with their respective coworkers),^{18,19} who were the first to demonstrate the potential of DNP as a method for improving NMR sensitivity in high-field liquid-state and solid-state studies, respectively. As a result, DNP

has emerged over the last few years as a very powerful method for enhancing NMR sensitivity, both in the liquid and in the solid states.^{20,21}

In DNP, the nuclear spin polarisation is enhanced by transferring the electron spin polarisation of paramagnetic species to nuclei *via* microwave irradiation at or near the electron Larmor frequency (*e.g.* ~263 GHz in a 9.4 T magnet), yielding a maximum increase in NMR signal intensity equal to the ratio of the electron to nucleus magnetogyric ratios (~660 for ¹H). The actual DNP efficiency is conventionally – although not quite correctly (*vide infra*) – quantified by considering the DNP signal enhancement (ϵ_{DNP}) defined as the ratio of the NMR signal intensities measured with (I_{ON}) and without (I_{OFF}) microwave irradiation ($\epsilon_{\text{DNP}} = I_{\text{ON}}/I_{\text{OFF}}$). The paramagnetic species required for DNP can either be *endogenous* (already present in the sample to analyse, either naturally or as a result of high-energy particle irradiation²²) or *exogenous* (added to the sample to analyse), and these paramagnetic species could potentially be stable or unstable (*e.g.* purposely generated prior to the NMR analysis with a correspondingly limited lifetime). The latter case is typically encountered in the field of chemically-induced DNP (CI-DNP),²³ which will not be covered by this contribution in which we will exclusively restrict ourselves to stable and (mostly) exogenous paramagnets. The chemical nature of these paramagnets, typically referred to as DNP polarising agents, has a strong influence on the type of DNP mechanism involved in the electron-to-nucleus DNP transfer, which itself depends also on the magnetic field strength at which experiments are performed. There are basically four main DNP mechanisms identified so far: the Overhauser Effect (OE), the Solid Effect (SE), the Cross Effect (CE), and the Thermal Mixing (TM).^{24,25} While these mechanisms have been the subject of extensive investigations, both at the early days of DNP and more recently,²⁶ there are still not completely understood, especially in the presence of magic-angle spinning (MAS).²⁷⁻³⁰ As such, it is important to distinguish between liquid-state DNP and solid-state DNP (with and without MAS), as the corresponding theory may be respectively different. In this review, we will focus exclusively on DNP SSNMR of solid-state samples

(predominantly with MAS). One can briefly mention, however, very interesting pieces of work where DNP in the liquid state has brought relevant information in the case of polymer materials.

For instance, Hilty and coworkers at Texas A&M University have published remarkable papers where they used the dissolution DNP (D-DNP) technique to study polymeric systems. In D-DNP, the nuclear polarisation of a given molecule first builds up by DNP in the solid state at extremely low temperatures (*ca.* 1–2 K) in a moderate magnetic field (*e.g.* 3–4 T), and then the resulting hyperpolarised solid is subsequently transferred to a higher magnetic field where it undergoes a very fast solid-to-liquid phase transition *via* its mixing with a super-heated solvent (a process that only slightly perturbs its strong hyperpolarisation) prior to being analysed at room temperature with a conventional high-field liquid-state NMR spectrometer.^{18,20} In particular, these authors used monomeric solutions hyperpolarized by D-DNP to detect key intermediates or highlight the polymer active site during polymerisation reactions,³¹ hereby illustrating the potential of the technique as a precious strategy to obtain real-time mechanistic and kinetic data on metallocene catalysis or ring-opening polymerisation.^{32,33} Second, Han and coworkers at the University of California, Santa Barbara, have strongly contributed to the use of the so-called low-field Overhauser liquid-state DNP (ODNP) technique as a way to probe and quantify the dynamics of hydration water locally (at the sub-nanometre scale).³⁴ In ODNP, a DNP polarising agent – usually referred to as a spin probe in this specific context – is added to the aqueous solution of interest, and its EPR transitions are saturated with microwaves to promote the DNP transfer from the unpaired electrons of the spin probe to the ¹H nuclei of the water molecules. The basic idea of the technique relies on the sensitivity of the DNP transfer efficiency to the local environment of the probe due to the time-dependence of the ¹H–electron dipolar coupling. These data can then be used to determine the local water translational diffusivity, which in turn informs on the local hydration dynamics. Strictly speaking, this approach clearly focuses on the elucidation of dynamic rather than structural features. However, site specificity can be achieved by analysing successively the water dynamic behaviour in a series of distinct cases where the spin probes are differently placed (*e.g.* covalently bound to different regions of the investigated macromolecule), so that the hydration water dynamics can be mapped out over the entire

system with spatial resolution. This is a very effective tool for probing the hydration water surrounding the surface and interface of macromolecules as well as for revealing macromolecular interactions. Originally applied with great success to the investigation of relevant biomacromolecules,³⁴ the approach was also shown to be very powerful for deciphering transport pathways in polymer membranes such as Nafion, one of the most common material used for proton exchange membranes in fuel cells.³⁵ Extension of the technique *via* the combination with fast field-cycling NMR relaxometry also appears quite promising.^{36,37}

Now, going back to DNP MAS SSNMR, the first applications to the analysis of polymer samples was due to the pioneering works of Wind and coworkers.³⁸ Initially driven by the need to characterise a series of coal samples, which intrinsically contained a substantial amount of unpaired electrons, these authors were confronted with ¹³C SSNMR MAS spectra with a very poor signal-to-noise ratio (S/N), and hence they investigated the possibility of using the endogenous paramagnets of the coals as a source for enhancing the S/N of their NMR spectra by DNP.^{39,40} Consequently, they constructed their own DNP MAS SSNMR instrumentation using a klystron as the microwave source.⁴¹ While this forced them to work at a relatively low magnetic field strength (1.4 T) in order to accommodate for the microwave frequency range accessible with klystron sources (≤ 40 GHz), they could still achieve remarkable results for the SSNMR analysis not only of coals,⁴² but also of diamonds⁴³ and, more relevant to the subject of this review, polymers.³⁸ In particular, they obtained the first 1.4 T DNP-enhanced ¹³C cross-polarisation (CP) MAS spectrum of a polymer sample, an atactic poly(styrene) doped with the monoradical BDPA (1,3-bisdiphenylene-2-phenyl allyl). In this respect, they compared the DNP signal enhancements obtained in DNP-enhanced ¹³C single-pulse excitation (SPE) MAS and ¹³C CP MAS experiments, and they showed that both schemes (referred to as direct and indirect ¹³C DNP, respectively) allowed significant improvement in terms of sensitivity per unit of time. Interestingly, they also observed that the ¹³C resonances in DNP-enhanced ¹³C SPE MAS spectra were relatively broader than those in DNP-enhanced ¹³C CP MAS spectra. They attributed this difference to the closer proximity between the unpaired electrons and the ¹³C spins for direct ¹³C DNP (where the ¹³C nuclei are necessarily located near the paramagnetic centres to allow the electron–¹³C DNP transfer to occur)

than for indirect ^{13}C DNP, where ^1H - ^1H spin diffusion may propagate the DNP-enhanced ^1H magnetisation away from the unpaired electrons prior to being transferred to ^{13}C spins by CP (hence resulting in ^{13}C signals whose linewidths are only weakly affected by the presence of the paramagnetic species in the sample). This early analysis is actually of fundamental importance because, depending on the structural heterogeneity of the analysed polymer material, DNP-enhanced ^{13}C CP or SPE MAS experiments may not necessarily reveal the same structural features, since they do not exactly probe the same length scales (*vide infra*). Wind and coworkers also used DNP for investigating undoped *trans*-polyacetylene,⁴⁴ an interesting example of a polymer containing endogenous unpaired electrons suitable for DNP. A few years later, Schaefer and coworkers went on to use DNP for studying selectively the interface in polymer blends, publishing a series of papers⁴⁵⁻⁴⁹ where they demonstrated that the selective paramagnetic doping of thick polymer films obtained through the serial film casting of immiscible polymers (at natural abundance or isotopically enriched), combined with NMR spectral differencing techniques, allowed for the detection of the NMR signals that were exclusively due to the polymer chains located at the interface of the blends.

While all these studies were, on their own, very inspiring, their true power for the detailed structural elucidation of solid-state polymer samples was invariably limited by the low magnetic field strength at which they were conducted. In this sense, a real breakthrough came in 1993 with the groundbreaking work by Griffin and Temkin at the Massachusetts Institute of Technology, who first proposed the use of continuous-wave gyrotrons as high-power/high-frequency microwave sources for DNP MAS SSNMR.¹⁹ Continuous gyrotrons are cyclotron resonance masers that can deliver high-frequency (≥ 200 GHz), high-power (≥ 50 W), continuous microwave irradiation over long periods of times (\sim days), which makes them ideally suitable to promote the electron-to-nucleus DNP transfer at high fields. In this paper, these authors used a similar sample to that used by Wind (poly(styrene) doped with BDPA)³⁸ and they obtained a ^{13}C DNP signal enhancement (ϵ_{DNP}) of 10 at room temperature. Likewise, they observed the same differences as Wind and coworkers in terms of ^{13}C signal linewidths for DNP-enhanced ^{13}C CP and SPE MAS spectra,

revealing the distinct characteristic length scales between indirect and direct ^{13}C DNP, respectively. In the following years, Griffin's group contributed with a series of impressive theoretical and technological achievements to the development of the DNP MAS SSNMR technique, opening up outstanding applications such as the analysis of relevant biological samples⁵⁰ including membrane proteins or amyloid fibrils.^{51,52} This trend has been further emphasised with the demonstration in 2010 by Emsley's and Bodenhausen's groups of its potential for the structural investigation of surfaces,⁵³ and the resulting advent of the so-called Surface Enhanced NMR Spectroscopy (SENS) technique.⁵⁴ The combination of all these remarkable results together with the commercial availability of the required high-field DNP MAS SSNMR instrumentation,⁵⁵ has brought solid-state DNP to the point where it has now achieved wide applicability. In this respect, many related reviews have been published over the past few years, dealing both with the theory and applications of the technique.^{21,54,56-64} In this respect, the comprehensive review by Corzilius and coworkers is one of the latest and very worth reading.⁶⁵ Therefore, considering the literature already available, the present contribution will purposely avoid discussing the latest theoretical and technological advances of DNP SSNMR (for which the interested reader is advised to consult the above-mentioned reviews), and will focus instead on the recent applications of the technique for the structural analysis of polymer materials, dealing first with the prerequisites for DNP MAS SSNMR and then describing a few selected pieces of work from the literature that are of relevance along these lines.

21.2. Implementing high-field DNP MAS SSNMR

For diamagnetic polymer materials, performing high-field DNP MAS SSNMR requires three basic ingredients: i) a DNP MAS SSNMR spectrometer equipped with a gyrotron, ii) an efficient DNP polarising agent, and iii) a reliable sample preparation method.

21.2.1. A high-field DNP MAS SSNMR spectrometer

To perform DNP MAS SSNMR at relatively high fields (>9 T), we need a high-field SSNMR spectrometer combined with a high-power/high-frequency microwave source that can continuously generate several tens

of watts of microwave power at frequencies of several hundreds of GHz.⁵⁵ Precisely, today, commercial DNP SSNMR spectrometers using gyrotron technology are available from 9.4 T up to 21.1 T corresponding to ¹H (and electron) Larmor frequencies of 400 MHz (263 GHz) and 900 MHz (591 GHz), respectively. Second, we need a low-temperature (LT) MAS probehead that can be used to perform DNP SSNMR experiments at cryogenic temperatures (~ 95 K – 110 K) under MAS. The use of cryogenic temperatures is indeed required as it decreases nuclear and electron relaxation rates, which in turn improves the DNP transfer efficiency. Commercial probeheads for NMR rotors from 3.2 mm (external diameter) down to 1.3 mm are nowadays available,⁶⁶ which allow maximum MAS rates from 15 kHz up to 40 kHz to be achieved, respectively. The continuous microwave beam generated by the gyrotron is propagated *via* a corrugated wave-guide from the gyrotron output to the sample inside the LT MAS probehead, which lies inside the bore of the superconducting magnet of the SSNMR spectrometer where the experiments are conducted. Therefore, similarly to D-DNP, two distinct superconducting magnets are needed: one for the gyrotron and another for the SSNMR spectrometer.¹⁸ Contrary to D-DNP, however, the NMR sample always remains inside the SSNMR spectrometer and it may be irradiated continuously by the microwave beam during the course of the SSNMR experiment.

21.2.2. An efficient DNP polarising agent

The efficiency with which DNP polarising agents contribute to the electron-to-nucleus DNP transfer (usually quantified by ϵ_{DNP}) depends on the DNP transfer mechanism at play, which itself is related to the molecular properties of the polarising agents. Therefore, the design and chemical synthesis of efficient DNP polarising agents has been the subject of extensive research over the last ten years, which has led from the use of nitroxide monoradicals (*e.g.* BDPA³⁸, TEMPO⁵⁰) to more complicated bisnitroxides with specific molecular weight and structural features.⁶⁷ In particular, Tordo and coworkers have introduced AMUPol⁶⁸ and TEKPol⁶⁹ – two of the most efficient DNP polarising agents at 9.4 T for aqueous and organic media, respectively – which can provide ϵ_{DNP} values of up to ~250 at 9.4 T and 100 K for model compounds, even

though recent work has shown that these DNP signal enhancements are in practice overestimated because of MAS-induced depolarisation effects.^{29,70} Their performance, however, dramatically drops (by 1 to 2 orders of magnitude) when the magnetic field or the temperature increases.⁷¹ For example, ϵ_{DNP} for AMUPol reduces to ~ 30 at 18.8 T and 100 K, or < 10 at 9.4 T and 160 K.⁶⁸ For highly challenging biomolecular samples, this may represent a serious issue because their detailed structural elucidation demands optimised spectral resolution, which typically requires the use of high magnetic fields (> 10 T) and relatively high temperatures (> 200 K).⁷² In contrast, for polymers, where the contribution to the spectral linewidth arises mainly from the inherent inhomogeneity of the sample (as in the case of amorphous polymers), going to the highest magnetic field strengths possible might not offer a significant advantage. The prospect to achieve large ϵ_{DNP} at high temperatures, however, would be particularly appealing, as it would open up the possibility to use DNP MAS SSNMR for the investigation not only of polymer *structure* but also of polymer *dynamics* (something that is nowadays unthinkable considering the cryogenic temperatures that are currently needed). Therefore, the main challenge at the moment in the field of DNP polarising agent design is the production of paramagnetic molecules that remain highly efficient at high magnetic fields and/or high temperatures,⁷³ and recent work illustrating the computationally assisted design of polarising agents gives hope in that direction.⁷⁴⁻⁷⁶

21.2.3. A reliable sample preparation method

Sample preparation is probably one of the most significant difficulties – not to say a possible *caveat* – of any DNP SSNMR experiment. As mentioned above, in order to perform DNP-enhanced SSNMR experiments on diamagnetic samples, they must be doped with a DNP polarising agent (typically of the order of $10 \mu\text{mol g}^{-1}$ for optimal results). In this context, one sample preparation method of choice is referred to in the literature as *incipient wetness impregnation*,⁵³ where a low amount of a radical-containing solution is used to impregnate the porous or extra-particle volume of the sample at room temperature (prior to being subjected to the DNP MAS SSNMR analysis at ~ 100 K). This method works remarkably well for porous

materials,⁵⁴ including for microporous organic polymers,⁷⁷ because the porous network allows the radicals to be (quite homogeneously) distributed inside the material, which is one of the key elements to the success of the SENS technique (which preferentially probes the material surface). For non-porous materials (such as organic powders), however, the radicals are invariably constrained at the surface of the particles, and hence whether or not the corresponding DNP MAS SSNMR experiment will be successful (*i.e.* observation of a large DNP signal enhancement) becomes critically dependent on the nuclear spin-lattice relaxation time (T_1) of the material. In other words, for indirect ^{13}C DNP (*i.e.* for DNP-enhanced ^{13}C CP MAS experiments), one should consider the ^1H spin-lattice relaxation time (or, more rigorously, the ^1H spin-lattice relaxation time measured with the microwave field *on*, thereafter referred to as $T_1[^1\text{H}]^{on}$). In particular, for organic powders with short $T_1[^1\text{H}]^{on}$ (<5 s), the incipient wetness impregnation method may either give deluding results or totally fail.⁷⁸ This is especially true for samples containing methyl groups whose rotational dynamics even at cryogenic temperatures provides an efficient relaxation sink under typical DNP MAS experimental conditions.^{79,80} In contrast, for long $T_1[^1\text{H}]^{on}$ values (> 100 s), Emsley and coworkers have shown that substantial DNP signal enhancements ($\epsilon_{\text{DNP}} > 50$ at 9.4 T) could be obtained because the long $T_1[^1\text{H}]^{on}$ values allowed significant ^1H - ^1H spin diffusion to occur, hereby relaying the enhanced ^1H polarisation from the surface to the bulk of the particle over micrometre length scales.⁷⁹ For polymer samples, this raises two issues. First, $T_1[^1\text{H}]^{on}$ values at ~ 100 K for polymers may be quite short (<10 s), which yields correspondingly low ϵ_{DNP} values.⁸⁰ Second, depending upon the structural heterogeneity of the investigated material, the resulting length scale over which the enhanced ^1H polarisation diffuses may prove insufficient to ensure that the resulting DNP MAS SSNMR spectrum does indeed represent a reliable signature of the whole molecular structure of the material. This (quite general) concern is actually captured perfectly by Saalwächter in the first Chapter of this book, when he writes: “*in a structurally (...) inhomogeneous sample, one inevitably has to worry whether the NMR method in question provides information that is representative of the whole sample or only a potentially ill-defined sub-ensemble.*” Therefore, alternative sample preparation methods for polymer materials have been investigated in the literature, including glass forming

or film casting. In both cases, the polymer is first solubilised in a radical-containing solution. For glass forming, low-temperature DNP MAS SSNMR experiments are directly recorded on the so-obtained frozen polymer solution, whereas, for film casting, the solvent is first evaporated and then the resulting powder-like sample is analysed. The performance of these methods has been assessed for a series of amorphous and semi-crystalline polymers of varying molecular weights, by comparing the sensitivity and resolution of ^{13}C CP MAS SSNMR experiments performed at 100 K with DNP with respect to their room-temperature (RT) counterparts without DNP. To properly compare the sensitivity in this case, it is critical not to focus only on ϵ_{DNP} , but to consider the *real* sensitivity enhancement that comes from using one instrumentation (LT, with DNP) in place of the other (RT, without DNP). There have been several studies in the literature dedicated to the adequate quantification of the real sensitivity gain brought about by DNP.⁸¹⁻⁸⁴ One possible indicator that we have used in our group is the so-called *absolute sensitivity ratio* (ASR) proposed by De Paëpe and coworkers,⁸³ which is defined as the ratio of the S/N of the LT DNP MAS SSNMR experiment to the S/N of the corresponding RT MAS SSNMR experiment without DNP. Overall, while both the glass forming and film casting sample preparation methods have their own advantages and disadvantages (*vide infra*), they do share the same strong limitation: they can only be applied to soluble polymers. Other sample preparation methods can also be envisioned, including matrix free⁸³ or spin labelling⁸⁴. This latter strategy was actually used recently in a very nice study by O'Dell and coworkers who synthesised nitroxides-containing polyurethanes with poly(ethylene oxide) (PEO) segments, which were subsequently studied by DNP-enhanced ^{13}C CP MAS SSNMR.⁸⁵ While these authors obtained relatively modest DNP signal enhancements (<15), they could elegantly apply a theoretical model proposed by Emsley and coworkers to probe the size and morphology of the crystalline PEO domains within the material,⁸⁶ obtaining a remarkable agreement with independent X-ray scattering data for one of the samples that displayed a lamellar morphology. All together, however, it should be kept in mind that no universal method is nowadays available to properly prepare *any* polymer sample for DNP analysis, at least as long as one seeks to optimise

both the sensitivity and the resolution of the experiment, especially for polymer samples with short ^1H spin-lattice relaxation times.

21.3. Using DNP MAS SSNMR for studying polymer materials

The original demonstrations of high-field DNP MAS SSNMR on polymers were concurrently reported by Viel's and Blanc's groups in 2013.^{77,78} The first study compared the outcomes of ^{13}C CP MAS SSNMR experiments recorded with DNP (at 110 K) with respect to their RT counterparts (without DNP) for a series of synthetic functional polymers, such as *living* polymers and macromonomers. Typically obtained by controlled radical polymerisation techniques, these macromolecules are quite remarkable because their chain end(s) can be involved in further polymerisation or chemical reactions, which opens up the possibility to synthesise macromolecular assemblies with complex architectures. Successful polymerisation with these techniques, however, requires a precise elucidation of the structure of the polymer chain ends in order to determine the quality of the control and exploit their reactivity. The challenge in this case comes from the low concentration of chain ends as compared to the polymer backbone, which results in weak NMR signals that can only be unequivocally detected under realistic experimental times if optimal sensitivity is achieved. For soluble polymers, one obvious choice for such characterisation would be to use liquid-state NMR. Reactive or fragile polymer end groups, however, are likely to react or degrade in solution over time, leading eventually to the detection of spurious NMR signals due to chemical moieties in the polymer structure that were not even present in the first place. This may be a major concern, for instance, for polymers obtained by nitroxide-mediated polymerisation (NMP), which relies on the reversible equilibrium between macroalkoxyamine and radical species resulting from the thermally labile C–ON bond.⁸⁷ Such acute thermal sensitivity also clearly precludes the use of another useful technique referred to in the literature as *melt-state* NMR,⁸⁸⁻⁹⁰ where the NMR analysis is conducted in the melt state at high temperature under MAS in order to achieve narrow NMR resonances with good S/N. In contrast, we showed that the use of DNP could provide more than an order of magnitude increase in absolute sensitivity with respect to RT experiments (**Figure 1**),

allowing ^{13}C CP MAS SSNMR spectra to be obtained on large molecular weight functional NMP-made polymers with very good sensitivity under reasonable experimental times (overnight).

[Figure 1 near here]

In other words, achieving the same results at RT without DNP would have required several months of uninterrupted acquisition time, which would have obviously been totally unrealistic. Similarly, we showed that this increase in sensitivity also allowed for the monitoring of chemical reactions involving the chain ends of large molecular weight NMP-made polymers,⁷⁸ an important point to assess when targeting multi-block copolymers with controlled molecular structures.

In the second study, DNP was shown to allow for the structural characterisation of microporous organic polymers (MOPs) in the solid state.⁷⁷ MOPs are promising materials that have been increasingly used in a wide variety of fields. While the detailed knowledge of their chemical structure is essential for optimising their functional properties, these materials are typically insoluble and amorphous, and hence both liquid-state NMR and X-rays crystallography cannot be used. In contrast, Blanc and coworkers showed how DNP could allow ^{13}C and ^{15}N CP MAS SSNMR spectra of a series of MOPs to be elucidated at natural abundance with speed and efficiency (**Figure 2**).

[Figure 2 near here]

These authors used incipient wetness impregnation with 1,1,2,2-tetrachloroethane as a solvent, achieving DNP signal enhancements in a magnetic field of 14.1 T of the order of 10. While the real gain in absolute sensitivity was not quantified, it is likely that, considering the systems under study, one order of magnitude increase in sensitivity was obtained (at least) with respect to RT MAS SSNMR analysis without DNP, which opens up the possibility to establish reliable structure-property relationship for these relevant materials.

Overall, when looking up at the recent literature (2013–2018) involving DNP SSNMR and polymer materials, except from a few studies that aim at understanding and optimising the DNP sensitivity

enhancements that were experimentally obtained, most reported studies invariably share the same driving force: deciphering structure-property in polymer materials. The following sections will review a few studies that belong to both categories.

On the one hand, regarding the optimisation of the DNP technique when applied to polymer materials, one can mention the works of Viel and coworkers^{80,91} who investigated and compared sample preparation methods for both amorphous and semi-crystalline polymer materials. Depending on the sample preparation method (film casting or glass forming), ASRs ranging from 4 to 40 were obtained in a magnetic field of 9.4 T at 110 K using TEKPol as a polarising agent (*ca.* 10 $\mu\text{mol g}^{-1}$) for a series of poly(styrene), poly(L-lactide), poly(L,D-lactide), poly(methyl methacrylate), or PEO of varying molecular weights (from 5 to 1 000 kg mol^{-1}) and synthesised by anionic polymerisation, ring-opening polymerisation, atom-transferred radical polymerisation, or NMP techniques. Results showed that, for amorphous polymers, the best method appeared to be glass forming because it invariably yielded the best sensitivity enhancements while preserving spectral resolution. For semi-crystalline polymers, however, the film casting method should be preferred. In fact, although providing lower sensitivity enhancements, this method allowed the spectral resolution to be reasonably maintained, as opposed to glass forming where resolution was significantly reduced owing to line broadening due to conformational distribution of the polymer chains in the frozen solution.⁸⁰ Further work showed that, in agreement with a previous report by Emsley and coworkers,⁹² DNP sensitivity enhancements obtained on polymers could be further increased by removing the adsorbed molecular oxygen (paramagnetic) from the DNP samples, especially for those polymers that display relatively high affinity towards O_2 (*e.g.* poly(styrene)).⁹¹ Finally, another study⁹³ revealed how dynamics at ~ 100 K could still have an impact and lead to misinterpretations of DNP-enhanced ^{13}C CP MAS SSNMR spectra as a result of differential magnetic relaxation properties. Precisely, analysis of methyl-containing polymers (*e.g.* poly(L-lactide), poly(L,D-lactide), poly(methyl methacrylate)) showed that the moderate increase in sample temperature observed at *ca.* 100 K when turning *on* the microwave irradiation (an increase that is typically lower than +10 K for non conductive species), still caused significant variations in

terms of CP dynamics that led to the observation of apparent non-uniform signal enhancements in the DNP-enhanced ^{13}C CP MAS SSNMR spectra (**Figure 3**).

[Figure 3 near here]

This intriguing phenomenon should clearly be accounted for when analysing polymer materials for which non-uniform DNP signal enhancements could possibly and legitimately be observed (*e.g.* for structurally heterogeneous polymer materials).

On the other hand, regarding the investigation of structure-property relationships in polymer materials, a few studies are very worth mentioning. First, Grey's group recently studied donor-acceptor stacking arrangements in bulk and thin-film conjugated polymers combining molecular modelling and DNP MAS SSNMR.⁹⁴ Conjugated polymers appear as promising alternatives in the field of semiconductors for a variety of reasons, the most significant of which being their remarkably high charge carrier mobilities. Tuning and optimising this fundamental property requires the molecular structure of these materials to be properly described and understood at the atomic level, both in the bulk and in thin-films, which is quite challenging due to their usual structural disorder (*i.e.* absence of long-range order). More specifically, these authors studied diketopyrrolo-pyrrole-dithienylthieno [3,2-b]thiophene (DPP-DTT) polymers combining density functional theory calculations and molecular dynamics simulations with multi-dimensional (1D, 2D) DNP MAS SSNMR experiments (**Figure 4**).

[Figure 4 near here]

In this way, they could determine the relative conformations and π - π stacking organisation of the DPP-DTT polymer backbone, both in the bulk and in thin films obtained by the drop-cast and spin-coated methods (with a minimal film thickness of 400 nm). The backbone structure of the DPP-DTT polymer was shown to be highly planar with donor and acceptor groups on adjacent chains in close proximity to one another, illustrating how the chemistry and conformation of the polymer backbone could be explicitly interrelated.

Quite remarkably, these authors also showed that the conformation of DPP-DTT in thin films was comparable to that observed in the bulk, thereby demonstrating the power of DNP MAS SSNMR for the structural elucidation of polymer thin films (which usually escape NMR analysis due to sensitivity issues).

The power of DNP for the SSNMR analysis of thin films was actually demonstrated also quite nicely in another study by Kaji and coworkers,⁹⁵ but using a different approach. Precisely, these authors used DNP-enhanced ³¹P static SSNMR to investigate the orientational analysis of amorphous phenyldi(pyren-1-yl)phosphine oxide (POPy₂), a semiconducting device used as an organic light-emitting diode with good electron transport properties. In contrast to angular-dependent photoluminescence measurements or variable-angle spectroscopic ellipsometry, which can only provide average values (*e.g.* order parameters), static SSNMR (*i.e.* without MAS) is in principle sensitive to molecular orientational distributions, but its low sensitivity precludes its uses in the case of thin films. These authors showed that this issue could be circumvented with DNP by analysing POPy₂ thin films vacuum-deposited or drop-cast onto SiO₂ substrates, and prepared with an appropriate amount of a selected DNP polarising agent. In this way, they obtained ³¹P chemical shift anisotropy (CSA) parameters that revealed clear orientation differences between both types of films (the former favouring a perpendicular orientation of the P=O axes to the SiO₂ substrates whereas the latter exhibited a random and isotropic distribution), which directly affected their photocurrent transient behaviours.

Moreover, building up on their previous (and above mentioned) work on MOPs characterisation, Blanc and coworkers have recently investigated the structure of amorphous photocatalytic polymers by one- (1D) and two-dimensional (2D) DNP MAS SSNMR experiments.⁹⁶ Organic polymeric photocatalysts have been shown to display a larger diversity than their metal-based counterparts, offering a promising alternative for the generation of hydrogen from water under illumination with the appropriate wavelength in the visible range. This study especially focused on copolymerised conjugated microporous polymers, which form 3D porous networks offering large surface areas and exhibiting remarkable hydrogen evolution rates (when

exposed to visible light). Similarly to MOPs, these insoluble polymers are largely amorphous, which prevents their analysis by liquid-state NMR, x-Rays, or even chromatography (for particle size determinations). In contrast, they can be efficiently characterised by DNP MAS SSNMR. In particular, the large sensitivity enhancements provided by DNP allowed 2D ^{13}C - ^{13}C INADEQUATE experiments to be recorded at natural abundance, yielding precise ^{13}C - ^{13}C connectivities that contributed irrefutably to the structural assignment. While very challenging to perform at natural abundance,⁹⁷ owing to the very low probability of having a pair of connected ^{13}C nuclei in a given molecule (of the order 0.01%), this powerful 2D experiment and – more generally – the actual determination of ^{13}C - ^{13}C connectivities^{79,83} and coupling constants⁹⁸, have become increasingly more common for solid-state samples at natural abundance thanks to DNP. Interestingly, Blanc and coworkers also implemented the so-called ^{13}C multiple cross-polarisation (multiCP) MAS technique,⁹⁹ which yield quantitative ^{13}C CP MAS SSNMR spectra in a very efficient manner provided that certain conditions are met (which were properly validated in their case). These quantitative data were compared with the monomer feed ratios used during the synthesis of COPs, which allowed the authors to confirm that the COPs networks were indeed concordant with the monomer stoichiometry. Alternatively, focusing again on polymer photocatalysts, another study by Hook and coworkers has recently revealed how DNP MAS SSNMR could be used to investigate the structure of metal-free polymeric carbon nitrides (PCNs),¹⁰⁰ which display promising photocatalytic properties including an apparent quantum efficiency of more than 50% for photocatalytic hydrogen evolution. Precisely, 1D and 2D ^{13}C or ^{15}N DNP MAS SSNMR experiments (including 2D ^{13}C - ^1H , ^{15}N - ^1H , or ^{13}C - ^{15}N correlation spectra) could be readily recorded on two selected PCN samples at natural abundance within realistic experimental times (**Figure 5**), showing in this case that a rich terminal N–H environment and an increased structural disorder were positively correlated with photocatalytic performance.

[Figure 5 near here]

The authors suggested that the presence of structural disorder may help introducing a trap state for the carriers that could compete with other trap states, which overall could provide new ideas for the synthesis of the next generations of PCN photocatalysts with improved performance.

21.4. Conclusion

DNP has brought a real revolution in the field of SSNMR leading to sensitivity enhancements that have made feasible SSNMR experiments that were totally unrealistic before. In the field of polymer materials, this paves the way to an improved understanding of structure-property relationships that are so eagerly required for optimising the performance of the materials or the devices (*e.g.* thin films). The need to incorporate DNP polarising agents within the materials, however, does remain a strong limitation because such incorporation may not always be physically possible (at least in a homogeneous manner) or it may alter the material morphology, which may lead to possible bias effects that could compromise the obtained structural data. Therefore, overcoming this challenge constitutes one of the main research priorities in order for this powerful technique to become increasingly more widespread in this exciting field.

Acknowledgement

This study has received funding from the Excellence Initiative of Aix-Marseille University - A*Midex, a French “Investissements d’Avenir” programme supported of the A*MIDEX project (no. ANR-11-IDEX-0001-02) funded by the “Investissements d’Avenir”, and from the European Research Council (ERC) under the European Union’s Horizon 2020 research and innovation programme (grant agreement No 758498).

References

1. M. R. Hansen, R. Graf and H. W. Spiess, *Chem. Rev.*, 2016, **116**, 1272.
2. H. W. Spiess, *Macromolecules*, 2017, **50**, 1761.
3. E. M. Purcell, H. C. Torrey and R. V. Pound, *Phys. Rev.*, 1946, **69**, 37.
4. F. Bloch, W. W. Hansen and M. Packard, *Phys. Rev.*, 1946, **69**, 127.
5. J. H. Ardenkjaer-Larsen, G. S. Boebinger, A. Comment, S. Duckett, A. S. Edison, F. Engelke, C. Griesinger, R. G. Griffin, C. Hilty, H. Maeda, G. Parigi, T. Prisner, E. Ravera, J. van Bentum, S. Vega, A. Webb, C. Luchinat, H. Schwalbe and L. Frydman, *Angew. Chem. Int. Ed.*, 2015, **54**, 9162.
6. A. W. Overhauser, *Phys. Rev.*, 1953, **92**, 411.
7. T. Carver and C. P. Slichter, *Phys. Rev.*, 1953, **92**, 212.
8. C. D. Jeffries, *Phys. Rev.*, 1957, **106**, 164.
9. A. Abragam, *Phys. Rev.*, 1955, **98**, 1729.
10. A. Abragam, *The principles of nuclear magnetism*, Oxford University Press, New York, 1961.
11. A. V. Kessenikh, V. I. Lushchikov, A. A. Manenkov and Y. V. Taran, *Sov. Phys. Solid State*, 1963, **5**, 321.
12. A. V. Kessenikh, A. A. Manenkov and G. I. Pyatnitskii, *Sov. Phys. Solid State*, 1964, **6**, 641.
13. C. F. Hwang and D. A. Hill, *Phys. Rev. Lett.*, 1967, **19**, 1011.
14. C. F. Hwang and D. A. Hill, *Phys. Rev. Lett.*, 1967, **18**, 110.
15. B. N. Provotorov, *Sov. Phys. JETP*, 1962, **14**, 1126.
16. M. Borghini, *Phys. Rev. Lett.*, 1968, **20**, 419.
17. M. Goldman, *Spin Temperature and Nuclear Magnetic Resonance in Solids*, Oxford University Press, Oxford, 1970.
18. J. H. Ardenkjaer-Larsen, B. Fridlund, A. Gram, G. Hansson, L. Hansson, M. H. Lerche, R. Servin, M. Thaning and K. Golman, *Proc. Natl. Acad. Sci. USA*, 2003, **100**, 10158.
19. L. R. Becerra, G. J. Gerfen, R. J. Temkin, D. J. Singel and R. G. Griffin, *Phys. Rev. Lett.*, 1993, **71**, 3561.
20. C. Griesinger, M. Bennati, H. M. Vieth, C. Luchinat, G. Parigi, P. Hofer, F. Engelke, S. J. Glaser, V. Denysenkov and T. F. Prisner, *Prog. Nucl. Magn. Reson. Spectrosc.*, 2012, **64**, 4.
21. Q. Z. Ni, E. Daviso, T. V. Can, E. Markhasin, S. K. Jawla, T. M. Swager, R. J. Temkin, J. Herzfeld and R. G. Griffin, *Acc. Chem. Res.*, 2013, **46**, 1933.
22. T. Kumada, Y. Noda and N. Ishikawa, *J. Magn. Reson.*, 2012, **218**, 59.
23. M. Goetz, in *Annu. Rep. NMR Spectrosc.*, ed. G. A. Webb, Elsevier Academic Press Inc, San Diego, 2009, vol. 66, pp. 77.
24. T. V. Can, Q. Z. Ni and R. G. Griffin, *J. Magn. Reson.*, 2015, **253**, 23.
25. T. Maly, G. T. Debelouchina, V. S. Bajaj, K. N. Hu, C. G. Joo, M. L. Mak-Jurkauskas, J. R. Sirigiri, P. C. A. van der Wel, J. Herzfeld, R. J. Temkin and R. G. Griffin, *J. Chem. Phys.*, 2008, **128**, 052211.
26. W. T. Wenckebach, *Essentials of Dynamic Nuclear Polarization*, Spindrift Publications, The Netherlands, 2016.
27. K. R. Thurber and R. Tycko, *J. Chem. Phys.*, 2012, **137**, 084508.
28. K. R. Thurber and R. Tycko, *J. Chem. Phys.*, 2014, **140**, 184201.
29. F. Mentink-Vigier, S. Paul, D. Lee, A. Feintuch, S. Hediger, S. Vega and G. De Paëpe, *Phys. Chem. Chem. Phys.*, 2015, **17**, 21824.
30. F. Mentink-Vigier, S. Vega and G. De Paëpe, *Phys. Chem. Chem. Phys.*, 2017, **19**, 3506.
31. Y. Lee, G. S. Heo, H. F. Zeng, K. L. Wooley and C. Hilty, *J. Am. Chem. Soc.*, 2013, **135**, 4636.
32. C. H. Chen, W. C. Shih and C. Hilty, *J. Am. Chem. Soc.*, 2015, **137**, 6965.
33. Y. Kim, C. H. Chen and C. Hilty, *Chem. Commun.*, 2018, **54**, 4333.
34. C. Y. Cheng and S. I. Han, in *Annu. Rev. Phys. Chem.*, eds. M. A. Johnson and T. J. Martinez, Annual Reviews, Palo Alto, 2013, vol. 64, pp. 507.

35. T. Uberruck, O. Neudert, K. D. Kreuer, B. Blumich, J. Granwehr, S. Stapf and S. Han, *Phys. Chem. Chem. Phys.*, 2018, **20**, 26660.
36. O. Neudert, C. Mattea, S. Stapf, M. Reh, H. W. Spiess and K. Munnemann, *Micropor. Mesopor. Mater.*, 2015, **205**, 70.
37. B. Gizatullin, O. Neudert, S. Stapf and C. Mattea, *ChemPhysChem*, 2017, **18**, 2347.
38. R. A. Wind, M. J. Duijvestijn, C. Vanderlugt, A. Manenschijn and J. Vriend, *Prog. Nucl. Magn. Reson. Spectrosc.*, 1985, **17**, 33.
39. R. A. Wind, J. Trommel and J. Smidt, *Fuel*, 1979, **58**, 900.
40. R. A. Wind, J. Trommel and J. Smidt, *Fuel*, 1982, **61**, 398.
41. R. A. Wind, F. E. Anthonio, M. J. Duijvestijn, J. Smidt, J. Trommel and G. M. C. Devette, *J. Magn. Reson.*, 1983, **52**, 424.
42. R. B. Jones, S. D. Robertson, A. D. H. Clague, R. A. Wind, M. J. Duijvestijn, C. Vanderlugt, J. Vriend and J. Smidt, *Fuel*, 1986, **65**, 520.
43. M. J. Duijvestijn, C. Vanderlugt, J. Smidt, R. A. Wind, K. W. Zilm and D. C. Staplin, *Chem. Phys. Lett.*, 1983, **102**, 25.
44. M. J. Duijvestijn, A. Manenschijn, J. Smidt and R. A. Wind, *J. Magn. Reson.*, 1985, **64**, 461.
45. M. Afeworki, R. A. McKay and J. Schaefer, *Macromolecules*, 1992, **25**, 4084.
46. M. Afeworki and J. Schaefer, *Macromolecules*, 1992, **25**, 4092.
47. M. Afeworki and J. Schaefer, *Macromolecules*, 1992, **25**, 4097.
48. M. Afeworki, S. Vega and J. Schaefer, *Macromolecules*, 1992, **25**, 4100.
49. M. Afeworki, R. A. McKay and J. Schaefer, *Mater. Sci. Eng. A-Struct. Mater. Prop. Microstruct. Process.*, 1993, **162**, 221.
50. D. A. Hall, D. C. Maus, G. J. Gerfen, S. J. Inati, L. R. Becerra, F. W. Dahlquist and R. G. Griffin, *Science*, 1997, **276**, 930.
51. Q. Z. Ni, T. V. Can, E. Daviso, M. Belenky, R. G. Griffin and J. Herzfeld, *J. Am. Chem. Soc.*, 2018, **140**, 4085.
52. K. K. Frederick, V. K. Michaelis, M. A. Caporini, L. B. Andreas, G. T. Debelouchina, R. G. Griffin and S. Lindquist, *Proc. Natl. Acad. Sci. USA*, 2017, **114**, 3642.
53. A. Lesage, M. Lelli, D. Gajan, M. A. Caporini, V. Vitzthum, P. Mieville, J. Alauzun, A. Roussey, C. Thieuleux, A. Mehdi, G. Bodenhausen, C. Copéret and L. Emsley, *J. Am. Chem. Soc.*, 2010, **132**, 15459.
54. A. J. Rossini, A. Zagdoun, M. Lelli, A. Lesage, C. Copéret and L. Emsley, *Acc. Chem. Res.*, 2013, **46**, 1942.
55. M. Rosay, L. Tometich, S. Pawsey, R. Bader, R. Schauwecker, M. Blank, P. M. Borchard, S. R. Cauffman, K. L. Felch, R. T. Weber, R. J. Temkin, R. G. Griffin and W. E. Maas, *Phys. Chem. Chem. Phys.*, 2010, **12**, 5850.
56. U. Akbey, W. T. Franks, A. Linden, M. Orwick-Rydmark, S. Lange and H. Oschkinat, in *Hyperpolarization Methods in Nmr Spectroscopy*, ed. L. T. Kuhn, 2013, vol. 338, pp. 181.
57. K. R. Thurber and R. Tycko, *Isr. J. Chem.*, 2014, **54**, 39.
58. T. Kobayashi, F. A. Perras, I. I. Slowing, A. D. Sadow and M. Pruski, *ACS Catal.*, 2015, **5**, 7055.
59. D. Lee, S. Hediger and G. De Paëpe, *Solid State Nucl. Magn. Reson.*, 2015, **66-67**, 6.
60. A. N. Smith and J. R. Long, *Anal. Chem.*, 2016, **88**, 122.
61. W. C. Liao, B. Ghaffari, C. P. Gordon, J. Xu and C. Coperet, *Curr. Opin. Colloid Interface Sci.*, 2018, **33**, 63.
62. L. Zhao, A. C. Pinon, L. Emsley and A. J. Rossini, *Magn. Reson. Chem.*, 2018, **56**, 583.
63. B. Bechinger, *Emagres*, 2018, **7**, 25.
64. F. A. Perras, T. Kobayashi and M. Pruski, *Emagres*, 2018, **7**, 35.
65. A. S. L. Thankamony, J. J. Wittmann, M. Kaushik and B. Corzilius, *Prog. Nucl. Magn. Reson. Spectrosc.*, 2017, **102**, 120.

66. S. R. Chaudhari, D. Wisser, A. C. Pinon, P. Berruyer, D. Gajan, P. Tordo, O. Ouari, C. Reiter, F. Engelke, C. Copéret, M. Lelli, A. Lesage and L. Emsley, *J. Am. Chem. Soc.*, 2017, **139**, 10609.
67. D. J. Kubicki, G. Casano, M. Schwarzwälder, S. Abel, C. Sauvee, K. Ganesan, M. Yulikov, A. J. Rossini, G. Jeschke, C. Copéret, A. Lesage, P. Tordo, O. Ouari and L. Emsley, *Chem. Sci.*, 2016, **7**, 550.
68. C. Sauvée, M. Rosay, G. Casano, F. Aussenac, R. T. Weber, O. Ouari and P. Tordo, *Angew. Chem. Int. Ed.*, 2013, **52**, 10858.
69. A. Zagdoun, G. Casano, O. Ouari, M. Schwarzwälder, A. J. Rossini, F. Aussenac, M. Yulikov, G. Jeschke, C. Copéret, A. Lesage, P. Tordo and L. Emsley, *J. Am. Chem. Soc.*, 2013, **135**, 12790.
70. F. Mentink-Vigier, G. Mathies, Y. Liu, A.-L. Barra, M. A. Caporini, D. Lee, S. Hediger, R. G. Griffin and G. De Paëpe, *Chem. Sci.*, 2017, **8**, 8150.
71. G. Mathies, M. A. Caporini, V. K. Michaelis, Y. Liu, K.-N. Hu, D. Mance, J. L. Zweier, M. Rosay, M. Baldus and R. G. Griffin, *Angew. Chem. Int. Ed.*, 2015, **54**, 11770.
72. U. Akbey and H. Oschkinat, *J. Magn. Reson.*, 2016, **269**, 213.
73. D. Wisser, G. Karthikeyan, A. Lund, G. Casano, H. Karoui, M. Yulikov, G. Menzildjian, A. C. Pinon, A. Porea, F. Engelke, S. R. Chaudhari, D. Kubicki, A. J. Rossini, I. B. Moroz, D. Gajan, C. Copéret, G. Jeschke, M. Lelli, L. Emsley, A. Lesage and O. Ouari, *J. Am. Chem. Soc.*, 2018, **140**, 13340.
74. F. Mentink-Vigier, I. Marin-Montesinos, A. P. Jagtap, T. Halbritter, J. van Tol, S. Hediger, D. Lee, S. T. Sigurdsson and G. De Paëpe, *J. Am. Chem. Soc.*, 2018, **140**, 11013.
75. F. A. Perras, A. Sadow and M. Pruski, *ChemPhysChem*, 2017, **18**, 2279.
76. F. A. Perras and M. Pruski, *J. Chem. Phys.*, 2018, **149**.
77. F. Blanc, S. Y. Chong, T. O. McDonald, D. J. Adams, S. Pawsey, M. A. Caporini and A. I. Cooper, *J. Am. Chem. Soc.*, 2013, **135**, 15290.
78. O. Ouari, T. Phan, F. Ziarelli, G. Casano, F. Aussenac, P. Thureau, D. Gigmes, P. Tordo and S. Viel, *ACS Macro Lett.*, 2013, **2**, 715.
79. A. J. Rossini, A. Zagdoun, F. Hegner, M. Schwarzwälder, D. Gajan, C. Coperet, A. Lesage and L. Emsley, *J. Am. Chem. Soc.*, 2012, **134**, 16899.
80. D. Le, G. Casano, T. N. T. Phan, F. Ziarelli, O. Ouari, F. Aussenac, P. Thureau, G. Mollica, D. Gigmes, P. Tordo and S. Viel, *Macromolecules*, 2014, **47**, 3909.
81. T. Kobayashi, O. Lafon, A. S. L. Thankamony, I. I. Slowing, K. Kandel, D. Carnevale, V. Vitzthum, H. Vezin, J. P. Amoureux, G. Bodenhausen and M. Pruski, *Phys. Chem. Chem. Phys.*, 2013, **15**, 5553.
82. A. J. Rossini, A. Zagdoun, M. Lelli, D. Gajan, F. Rascon, M. Rosay, W. E. Maas, C. Coperet, A. Lesage and L. Emsley, *Chem. Sci.*, 2012, **3**, 108.
83. H. Takahashi, D. Lee, L. Dubois, M. Bardet, S. Hediger and G. De Paëpe, *Angew. Chem. Int. Ed.*, 2012, **51**, 11766.
84. V. Vitzthum, F. Borcard, S. Jannin, M. Morin, P. Mieville, M. A. Caporini, A. Sienkiewicz, S. Gerber-Lemaire and G. Bodenhausen, *ChemPhysChem*, 2011, **12**, 2929.
85. E. Verde-Sesto, N. Goujon, H. Sardon, P. Ruiz, T. V. Huynh, F. Elizalde, D. Mecerreyes, M. Forsyth and L. A. O'Dell, *Macromolecules*, 2018, **51**, 8046.
86. A. C. Pinon, J. Schlagnitweit, P. Berruyer, A. J. Rossini, M. Lelli, E. Socie, M. X. Tang, T. Pham, A. Lesage, S. Schantz and L. Emsley, *J. Phys. Chem. C*, 2017, **121**, 15993.
87. J. Nicolas, Y. Guillaneuf, C. Lefay, D. Bertin, D. Gigmes and B. Charleux, *Prog. Polym. Sci.*, 2013, **38**, 63.
88. M. Pollard, K. Klimke, R. Graf, H. W. Spiess, M. Wilhelm, O. Sperber, C. Piel and W. Kaminsky, *Macromolecules*, 2004, **37**, 813.
89. K. Klimke, M. Parkinson, C. Piel, W. Kaminsky, H. W. Spiess and M. Wilhelm, *Macromol. Chem. Phys.*, 2006, **207**, 382.
90. F. J. Stadler, C. Piel, K. Klimke, J. Kaschta, M. Parkinson, M. Wilhelm, W. Kaminsky and H. Munstedt, *Macromolecules*, 2006, **39**, 1474.

91. D. Le, F. Ziarelli, T. N. T. Phan, G. Mollica, P. Thureau, F. Aussenac, O. Ouari, D. Gigmes, P. Tordo and S. Viel, *Macromol. Rapid Comm.*, 2015, **36**, 1416.
92. D. J. Kubicki, A. J. Rossini, A. Porea, A. Zagdoun, O. Ouari, P. Tordo, F. Engelke, A. Lesage and L. Emsley, *J. Am. Chem. Soc.*, 2014, **136**, 15711.
93. G. Mollica, D. Le, F. Ziarelli, G. Casano, O. Ouari, T. N. T. Phan, F. Aussenac, P. Thureau, D. Gigmes, P. Tordo and S. Viel, *ACS Macro Lett.*, 2014, **3**, 922.
94. S. R. Chaudhari, J. M. Griffin, K. Broch, A. Lesage, V. Lemaur, D. Dudenko, Y. Olivier, H. Siringhaus, L. Emsley and C. P. Grey, *Chem. Sci.*, 2017, **8**, 3126.
95. K. Suzuki, S. Kubo, F. Aussenac, F. Engelke, T. Fukushima and H. Kaji, *Angew. Chem. Int. Ed.*, 2017, **56**, 14842.
96. N. J. Brownbill, R. S. Sprick, B. Bonillo, S. Pawsey, F. Aussenac, A. J. Fielding, A. I. Cooper and F. Blanc, *Macromolecules*, 2018, **51**, 3088.
97. A. Lesage, C. Auger, S. Caldarelli and L. Emsley, *J. Am. Chem. Soc.*, 1997, **119**, 7867.
98. G. Mollica, M. Dekhil, F. Ziarelli, P. Thureau and S. Viel, *Angew. Chem. Int. Ed.*, 2015, **54**, 6028.
99. R. L. Johnson and K. Schmidt-Rohr, *J. Magn. Reson.*, 2014, **239**, 44.
100. X. B. Li, I. V. Sergeev, F. Aussenac, A. F. Masters, T. Maschmeyer and J. M. Hook, *Angew. Chem. Int. Ed.*, 2018, **57**, 6848.

Figure Captions

Figure 1. ^{13}C CP MAS SSNMR spectra of a *living* NMP-made poly(styrene) sample ($M_n = 13.5 \text{ kg mol}^{-1}$) obtained (a) without or (b) with DNP (at 285 K and 105 K, respectively). The sample in (b) was doped with a selected polarising agent (bCTbK)⁶⁷ at 0.5 wt %. In both cases, about 26k scans were accumulated and intensity scales are identical. The inset in (a) shows the corresponding molecular structure with the expected chain ends. Reprinted with permission from reference [78]. Copyright 2013 American Chemical Society.

Figure 2. (a) Molecular structures and general reaction scheme associated with the families of MOPs (referenced as **P1-R-X**) considered in the study by Blanc and coworkers,⁷⁷ with R the functional mononitrile aromatic compound and X the feed molar ratio (15% or 30%) used in the MOPs synthesis. (b,c) DNP-enhanced ^{15}N CP MAS SSNMR spectra recorded for samples (b) **P1-NH₂-15** and (c) **P1-NH₂-30** at natural abundance (0.37% for ^{15}N), which clearly show distinct ^{15}N resonances due to the nitrogens of the triazine, 4-aminobenzene, and 4-cyanobenzene moieties (at 252 ppm, 66 ppm, and 125 ppm, respectively). The labels “*” denote spinning sidebands. Adapted with permission from reference [77]. Copyright 2103 American Chemical Society.

Figure 3. (a) ^{13}C CP MAS SSNMR spectra recorded at cryogenic temperatures with DNP (green) and without DNP (red) on a poly(D,L-lactide) sample prepared by film casting (with TEKPol). The different temperatures observed in both cases (110 K and 100 K, respectively) simply result from microwave-induced heating of the sample as the microwave field is either turned *on* and *off*, respectively. An apparently larger ϵ_{DNP} value is clearly obtained for the ^{13}C NMR resonance due to the CH_3 groups with respect to the other two resonances (due to the CH and CO groups). (b) ^{13}C CP MAS buildup curves of the CH_3 group obtained for the same sample as a function of the CP contact time for the same two temperatures (100 K and 110 K). Here, however, the microwave field was voluntarily turned *off* and the sample temperature was adjusted simply by controlling the temperature of the MAS gases. The change in temperature clearly has a strong

impact on the CP buildup curves of the CH₃ groups (an observation that was also true for the CH and CO resonances, although to a lesser extent). Adapted with permission from reference [93]. Copyright 2014 American Chemical Society.

Figure 4. (a) 9.4 T ¹³C CP MAS SSNMR spectra of a bulk DPP-DTT sample prepared by incipient wetness impregnation using 1,1,2,2-tetrachloroethane-*d*₂ and TEKPol, recorded with the microwave field (μ W) turned *on* and *off* (upper and lower spectra, respectively). Note that all samples in (b-d) were prepared as in (a). (b,c) 9.4 T DNP-enhanced 2D ¹H-¹³C HETCOR MAS SSNMR spectra of 2 distinct DPP-DTT samples: (b) bulk polymer and (c) drop-cast film. (d) 9.4 T DNP-enhanced ¹³C CP MAS SSNMR spectra of drop-cast (red) and spin-coated (blue) DPP-DTT films. For spectral assignment, please refer to the original work. Adapted from reference [94] with permission from The Royal Society of Chemistry.

Figure 5. 9.4 T DNP-enhanced 2D ¹³C-¹⁵N correlation spectrum of a metal-free polymeric carbon nitride impregnated with a glycerol/water mixture containing AMUPol. The labels “*imp*” and “*” refer to impurities and MAS spinning sidebands, respectively. Adapted with permission from reference [100]. Copyright 2018 Wiley.

Figure 1

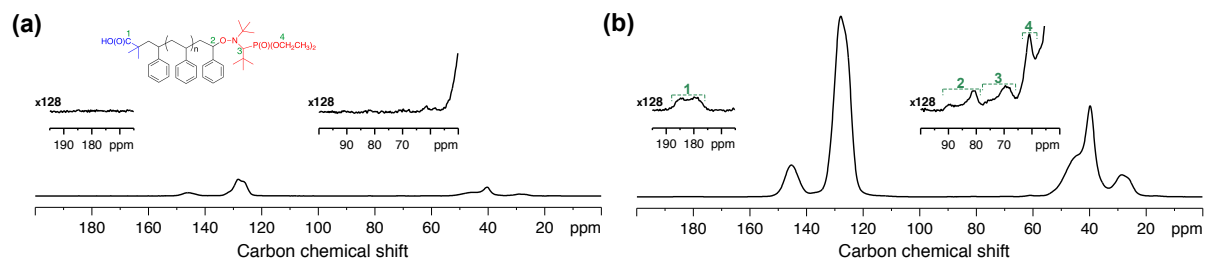


Figure 2

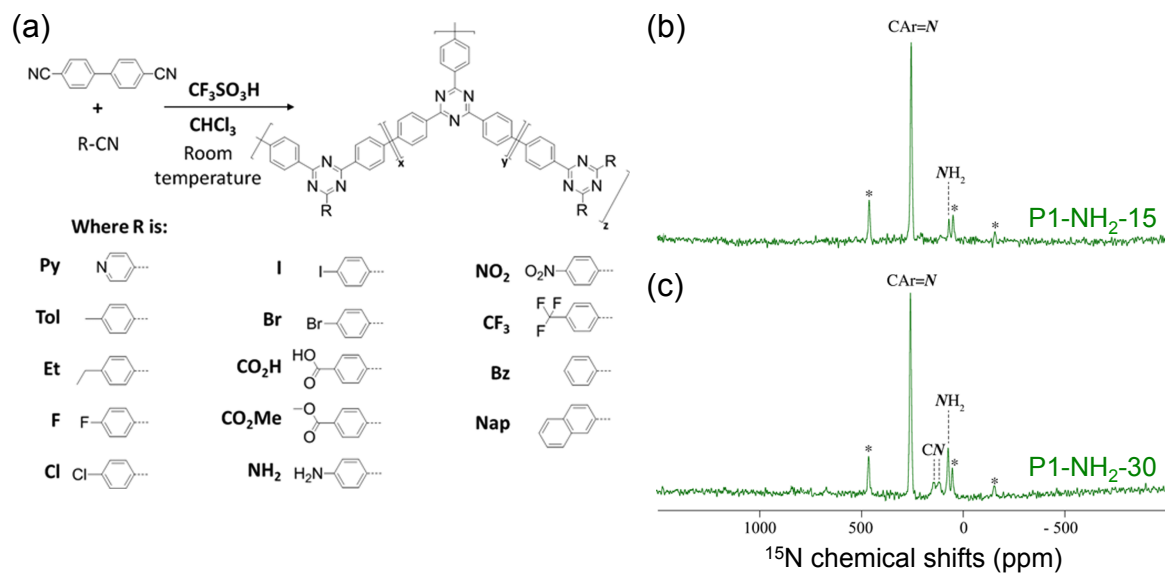


Figure 3

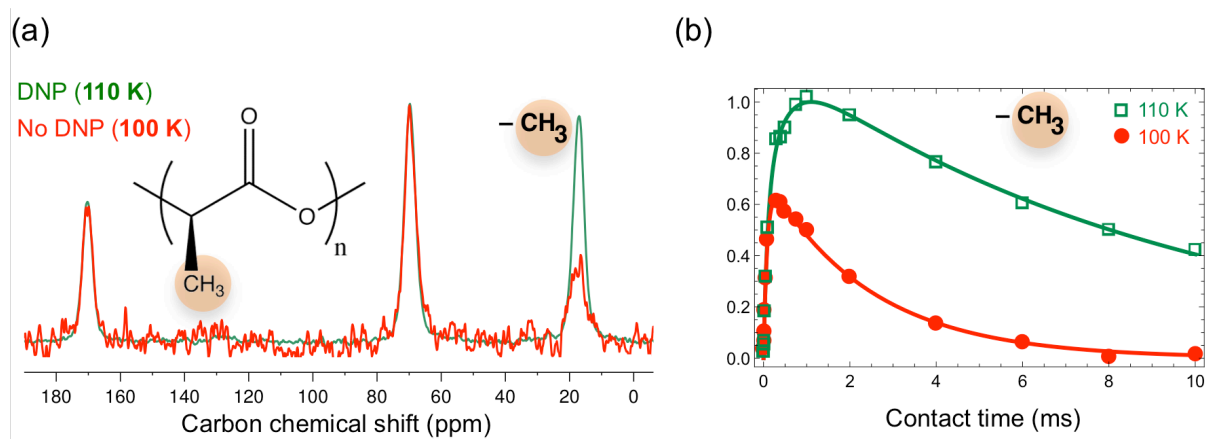


Figure 4

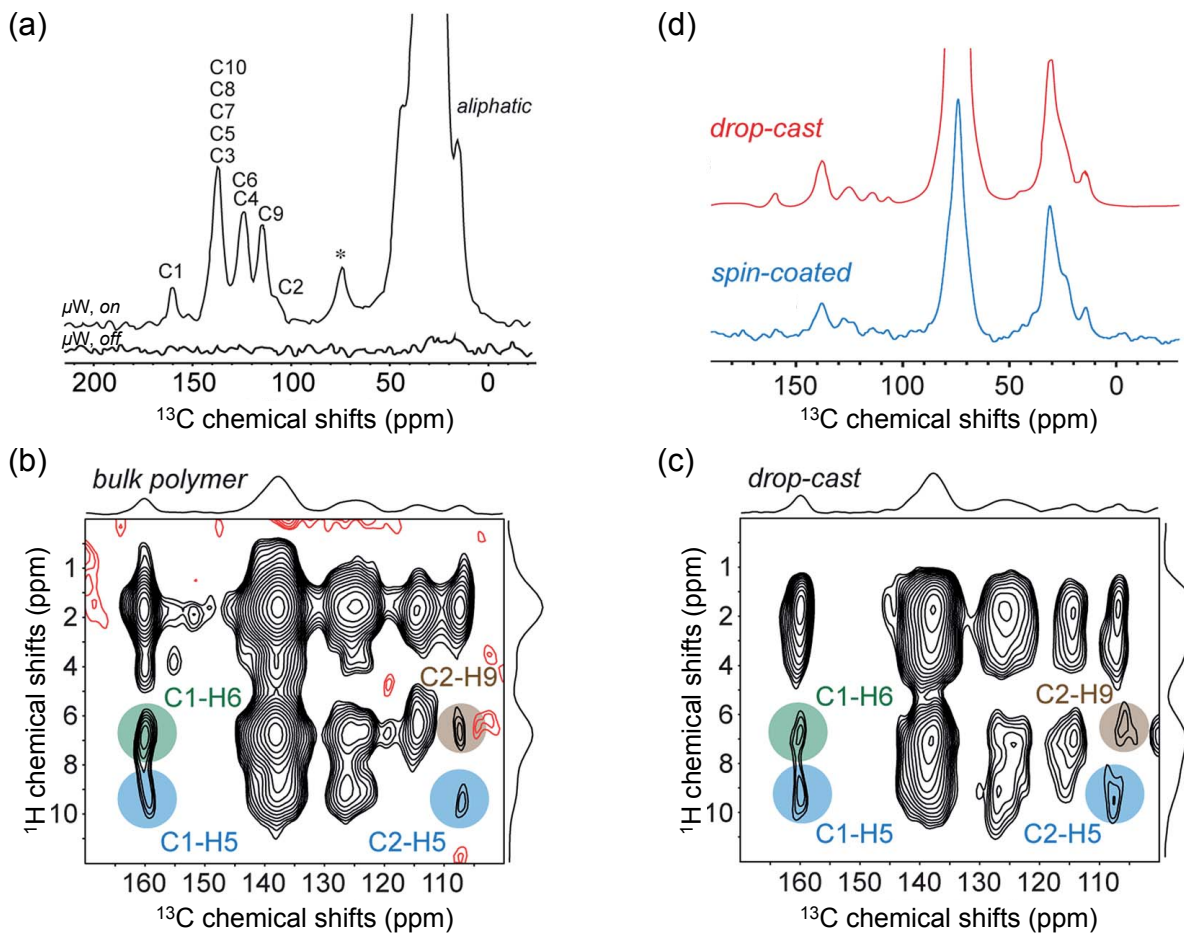


Figure 5

